Plant Cell Reports (2026) 45:82
https://doi.org/10.1007/s00299-026-03763-3

ORIGINAL ARTICLE

Comparative proteomics provides Insights into activation of jasmonic acid-mediated resistance mechanism in chickpea–*Helicoverpa armigera* interaction

Gothe Revanayya[1,2] · Inderjit Singh[1] · Onkarappa Dhanyakumar[2,3] · Jagdish Jaba[2] · Dharminder Bhatia[1] · Shayla Bindra[1] · Ravinder Singh[1] · Himabindu Kudapa[2] · Kalenahalli Yogendra[2]

Received: 27 October 2025 / Accepted: 24 February 2026 / Published online: 10 March 2026

Abstract

Key Message **Integrated host–pest proteomics revealed that chickpea resistance to *Helicoverpa armigera* involves early jasmonic acid signaling and linoleic acid–derived pro-toxins from crop wild relatives, providing molecular targets for breeding insect-resilient cultivars.**

Abstract Chickpea (*Cicer arietinum* L.), being a vital food legume, suffers severe yield reductions due to the pod borer *Helicoverpa armigera*. Despite extensive breeding efforts, durable resistance has remained elusive due to limited insights into the molecular basis of host–pest interactions. To address this gap, a first-of-its-kind integrated host–pest proteomic analysis in chickpea was performed to unravel the molecular mechanisms underlying natural insect resistance. Using untargeted LC–MS/MS, the proteomes resistant (ICCV506EB), susceptible (ICC3137) and a resistant crop wild relative (CWR's) (IG73016, *C. cuneatum*), along with larvae feeding on these genotypes, were simultaneously profiled. Resistant genotypes elicited a rapid, multi-layered defense response involving jasmonic acid (JA)-mediated signaling, transcriptional reprogramming, and fatty acid–derived secondary metabolites. In turn, *H. armigera* activated detoxification enzymes, proteolytic modulation, and behavioral countermeasures. Strikingly, larvae feeding on resistant CWRs failed to overcome defenses, as linoleic acid (LA) derivatives are suggested to act as pro-toxin-like factors, adversely affecting larval survival, digestion, growth, and development. The findings reveal the dynamic defense–counter-defense interplay between chickpea and *H. armigera*. This interplay highlights the key biomolecular nodes associated with durable resistance. This study provides correlative evidence suggesting that LA-derived defense metabolites may function as potential pro-toxin-like compounds and establishes CWRs as a rich source of resistance traits. Importantly, enhancing early JA-pathway activation through molecular breeding or biotechnology could accelerate the development of insect-resilient chickpea cultivars, thereby boosting crop productivity and sustainability.

Keywords Chickpea · Crop wild relatives · Fatty acid · *Helicoverpa armigera* · Jasmonic acid · Proteomics

Introduction

The pod borer, *Helicoverpa armigera* Hüb. (Lepidoptera: Noctuidae), is one of the most destructive global insect pests of chickpea (*Cicer arietinum* L.), causing major yield losses that may reach 50–90% (Sharma et al. 2007; Jaba et al. 2017; War et al. 2024). Current management practices rely predominantly on synthetic insecticides. However, their extensive use has resulted in the rapid flare-up of insecticide resistance and severe ecological consequences (Aboua et al. 2010). These limitations highlight the necessity for sustainable and environmentally compatible pest management strategies. Host plant resistance (HPR) offers a promising approach, providing an eco-friendly means to mitigate crop damage (Golla et al. 2018b). Nevertheless, resistance levels in cultivated chickpea remain low to moderate, whereas several crop wild relatives (CWRs), including *C. bijugum*, *C. judaicum*, and *C. cuneatum*, exhibit substantial resistance to *H. armigera*, representing valuable reservoirs of resistance genes (Golla et al. 2018b). Conventional breeding efforts to introgress these traits are constrained by sexual incompatibility and high autogamy in chickpea (Somers et al. 2003). This highlights the need for alternative strategies to harness the genetic potential of wild relatives.

Communicated by Neal Stewart.

Extended author information available on the last page of the article

Although wild relatives of chickpea represent valuable reservoirs of resistance against pod borer, the molecular basis of this resistance remains poorly understood till date. Previous studies have largely emphasized assessments of morphological and basic biochemical characterization, with comparatively limited exploration of molecular-level mechanisms to accelerate resistance gene discovery for facilitating targeted breeding. Recent advances in multi-omics technologies have greatly improved our understanding of plant–insect interactions in legumes, offering novel avenues to unravel the molecular determinants of resistance (Golla et al. 2018a, 2020; Jaba et al. 2021; Gothe et al. 2024). These approaches have already elucidated complex defense signaling pathways and stress-responsive networks in other crop systems (Yogendra et al. 2017; Avuthu et al. 2024). Among these, comparative proteomics has emerged as a powerful tool, enabling the identification and quantification of differentially expressed proteins during insect herbivory, thereby revealing key enzymes and regulatory components that orchestrate host defense responses (Rustagi et al. 2021; Pavithran et al. 2024).

Notably, comparative proteomics provides critical insights into how resistant plants deploy defense responses that impair herbivore growth and survival. In chickpea, proteins such as mannitol dehydrogenase (MADH), CSA1, serine/threonine kinase D6PKL2, and reactive oxygen species (ROS)-scavenging enzymes have been found to be accumulated in the genotypes fed by *H. armigera* (Bhattacharjee et al. 2020). Parallel studies in pigeonpea and rice further demonstrate that resistant genotypes consistently upregulate antioxidants and secondary metabolic pathways to restrict herbivory (Cheah et al. 2020; Ngugi-Dawit et al. 2021). Similarly, in sorghum, resistant genotypes exposed to stem borer attack exhibited enhanced stress-responsive and metabolic proteins associated with reduced insect performance (Tamhane et al. 2021). Conversely, *H. armigera* secretes salivary effectors such as glucose oxidase to suppress host defenses (Celorio-Mancera et al. 2011), while plant toxins trigger detoxification enzymes like glutathione S-transferases (Zheng et al. 2022). Despite these insights, most studies have focused on either plant or insect proteomics in isolation, with limited integration of both perspectives, representing a critical gap in fully dissecting the molecular mechanisms at the plant–insect interface.

To address this gap, in this study, untargeted Liquid Chromatography – Tandem Mass Spectrometry (LC–MS/MS) was performed to simultaneously profile proteomes of contrasting chickpea genotypes, including cultivated and its wild relative, together with *H. armigera* larvae feeding on them. Proteolytic interactions were further validated through molecular docking, simulation, and insect bioassays. The integrated analyses uncovered a molecular tug-of-war in which the resistant wild relative reinforces its defense network, severely impairing larval growth, development, and survival, while the insect attempts to reconfigure its digestive and detoxification machinery—yet ultimately fails. This dual proteomics strategy provides a holistic view of resistance-associated proteins in chickpea and their inhibitory effects on the insect gut, offering novel mechanistic insights into host defense and pest mortality.

Materials and methods

Plant materials

Cultivated chickpea (*C. arietinum*) genotypes ICCV 506 EB (Resistant) and ICC 3137 (Susceptible) were chosen based on their well-characterized resistance profiles (Gowda et al. 1983; Narayanamma et al. 2013). In addition, wild relative *C. cuneatum* (IG 73016) was selected as a promising source of resistance based on extensive pod bioassay under controlled lab conditions at both Punjab Agricultural University (PAU), Ludhiana, India, and International Crops Research Institute for the Semi-Arid Tropics (ICRISAT), Patancheru, India. All seed material was obtained from the Genebank of the ICRISAT, Patancheru, India. Plants were grown in a controlled glasshouse conditions with maintained at 27 ± 1 °C, 70 ± 10% relative humidity, with an 18:6 h light–dark photoperiod to ensure uniform growth and timely transition to the reproductive stage.

Artificial infestation and sample collection

Half-seed-filled chickpea pods were selected from the contrasting chickpea genotypes grown under glasshouse conditions, and late third-instar larvae were introduced and covered with clip cages (5×1.5 cm) to restrict larval feeding and movement. The 24 h post-infestation (hpi) time point was selected based on a preliminary pilot experiment conducted using the susceptible check genotype, which showed clear feeding damage and a measurable early defense response at this stage. This time point was intended to capture early host-insect interaction events. After 24 hpi, the clip cages were carefully opened, and the infested pods were excised from the plants using sterilized scissors. These pod samples were then collected and stored at −80 °C until further processing for protein extraction and analysis. Simultaneously, the *H. armigera* larvae released on different genotypes were removed using forceps and collected separately. Further, the midguts of larvae fed on different genotypes were dissected separately, collected in 1X PBS buffer (pH 7.0), and stored at −80 °C (Fig. S3).

Plant protein extraction

Proteins were extracted from chickpea pod tissues using a phenol-based protocol (Bhatnagar et al. 2021). Approximately 150 mg of frozen pods (three biological replicates) were ground in liquid nitrogen and homogenized in extraction buffer [0.9 M sucrose, 0.1 M Tris–HCl (pH 8.8), 10 mM EDTA, 50 mM DTT, 1 mM (PhenylMethylSulfonyl Fluoride) PMSF, and protease inhibitor cocktail (Sigma-Aldrich, USA)]. An equal volume of Tris-saturated phenol was added, and samples were incubated at 4 °C for 30 min with shaking. After centrifugation (5000 rpm, 20 min, 4 °C), the phenolic phase was collected and re-extracted twice with buffer/phenol. Proteins were precipitated with five volumes of 0.1 M ammonium acetate containing 10 mM DTT and incubated at − 80 °C overnight. The resulting pellet was centrifuged (5000 rpm, 30 min, 4 °C), washed twice with cold methanol (10 mM DTT) and once with cold acetone (10 mM DTT), and finally dissolved in rehydration buffer (8 M urea, 4% CHAPS, 40 mM Tris-base) or stored at − 80 °C until further use.

Insect gut protein extraction

The *H. armigera* gut was homogenized in 1X PBS buffer using a micro pestle and mortar. The homogenate was lysed in 200 µL of dissolution buffer containing 50 mM Tris–Cl (pH 8.0), 8 M urea, 2 M thiourea, 2 M EDTA, and a 1 × protease inhibitor cocktail (Sigma-Aldrich, St. Louis, MO, USA). Subsequently, 800 µL of ice-cold acetone supplemented with 10 mM dithiothreitol (DTT) was added. The samples were incubated at − 20 °C for 2 h to facilitate protein precipitation. After incubation, the samples were centrifuged at 12,000 rpm for 20 min at 4 °C. The resulting protein pellets were collected and washed twice with 800 µL of ice-cold acetone (Zheng et al. 2021). Finally, the pellets were either dissolved in rehydration buffer (8 M urea, 4% CHAPS w/v, 40 mM Tris-base) or stored at − 80 °C until further use.

In-solution digestion of plant and insect proteins

Protein concentrations were quantified using a Qubit fluorometer (Life Technologies, Malaysia software version APP v0.66 + MCU v0.20) prior to digestion. Equal volumes of protein extracts and RapiGest SF prepared in ammonium bicarbonate were incubated at 65 °C for 30 min for denaturation. Disulfide bonds were reduced with 10 µL of 100 mM dithiothreitol (DTT) at 65 °C for 30 min, followed by alkylation with 20 µL of 100 mM iodoacetamide (IAM) in the dark at room temperature for 30 min. Proteins were digested overnight at 37 °C using trypsin at a 1:20 enzyme-to-protein ratio. Digestion was stopped by adding formic acid (5% v/v), and samples were dried by vacuum centrifugation. Peptides were reconstituted in 10–20 µL of 0.1% formic acid, cleaned using ZipTip (Millipore), and used for LC–MS/MS analysis.

Mass spectrometry and data acquisition

Tryptic peptides were reconstituted in 50 µL of 0.1% formic acid and separated using an Acquity BEH C18 UPLC column (75 µm × 150 mm, 1.7 µm; Waters, UK) on a UPLC system. Peptides were resolved over 90 min with a binary gradient of solvent A (0.1% formic acid in water) and solvent B (0.1% formic acid in acetonitrile), increasing B from 53 to 85%. The flow rate was set at 5 µL/min for the initial 3 min (equilibration) and then increased to 200 µL/min. Column temperature was maintained at 60 °C. Eluted peptides were analyzed using a UPLC-Xevo-G2-XS-Q-TOF mass spectrometer (Waters, USA) with an electrospray ionization source in positive mode. Data were acquired in resolution mode with a 0.5 s scan across m/z 50–2000 Da. Instrument settings included a cone voltage of 40 V, low-energy trap/transfer voltages of 4 V, and a high-energy trap collision energy ramp from 15 to 40 V. Leucine enkephalin (200 pg/µL; Sigma-Aldrich, USA) was used as an external calibrant, with lock mass correction applied every 30 s. Data were processed using MassLynx v4.0 software, followed by protein identification and expression profiling (Bhatnagar et al. 2021).

LC–MS/MS raw data processing

Raw MS/MS data were processed in Progenesis QI for Proteomics v4.0 (Nonlinear Dynamics), with retention time alignment across runs to generate peak lists of *m/z* values and intensities. Ions with charge states ≥ + 5, retention times of 5–80 min, and *m/z* range of 100–1600 were considered. Samples (triplicate per treatment) were normalized prior to relative abundance comparisons, and peptides mapping to multiple proteins were excluded to ensure quantification accuracy.

Protein identification was carried out using the ion accounting algorithm against UniProt databases of *Cicer arietinum* and *H. armigera*. In cases where chickpea-specific annotation was limited, homology-based functional assignments were supported using the closely related species *Glycine max*. Search parameters included trypsin digestion (≤ 2 missed cleavages), 20 ppm precursor mass tolerance, and minimum thresholds of two fragment ions per peptide, five per protein, and at least two unique peptides per protein. Carbamidomethylation of cysteine was set as a fixed modification, while methionine oxidation and N-terminal pyroglutamate formation were specified as variable modifications. False discovery rate (FDR) was controlled at ≤ 5% using the Benjamini–Hochberg procedure (Benjamini and Hochberg

1995). Proteins with ≥ 2 unique peptides were retained for quantitative analysis.

Relative expression profiles of candidates from proteomics data

Total RNA was extracted from frozen pod samples of both *H. armigera*-infested and *H. armigera*-uninfested samples collected 24 hpi using the RNeasy Plant Mini Kit (Qiagen), with three biological replicates. Approximately 2.0 µg of purified RNA from each sample was used for cDNA synthesis, following the manufacturer's instructions (Thermoscript RT-PCR System, Invitrogen). Quantitative real time-PCR (qRT-PCR) was performed using gene-specific primers (Table S1) on a CFX96™ Real-Time PCR System (Bio-Rad). Cycle threshold (Ct) values were normalized against the housekeeping gene *actin*, and relative gene expression levels were calculated using the $2^{-\Delta\Delta Ct}$ method (Livak and Schmittgen 2001).

Protein–ligand molecular docking of linoleic acid with CYP450 in *H. armigera*

Linoleic acid, identified from the fatty acid biosynthesis pathway in resistant chickpea genotypes, was selected for molecular docking. Its 3D structure (PubChem CID: 5,280,450) was retrieved from PubChem. The *H. armigera* CYP450 proteome sequence (AAR37015.1) was retrieved from NCBI and modeled via SWISS-MODEL using the closest insect CYP450 template with 99.06% sequence identity. Model quality was evaluated using PROCHECK (https://saves.mbi.ucla.edu/), and the stereochemical properties were confirmed by Ramachandran analysis.

Docking was performed in PyRx 0.8 (AutoDock Vina). The modeled CYP450 structure was prepared with polar hydrogens, Gasteiger charges, and merged non-polar hydrogens; ligand rotatable bonds were automatically assigned. The geometry of linoleic acid was optimized using the Universal Force Field (UFF). Docking results were expressed as binding affinities (kcal/mol), where more negative values indicated stronger binding. Protein–ligand complexes were visualized in BIOVIA Discovery Studio to identify hydrogen bonding, hydrophobic interactions, and active site residues.

Molecular dynamics (MD) simulations of linoleic acid–CYP450 complex

Molecular dynamics (MD) simulations were performed to assess the stability and dynamic behavior of the linoleic acid–CYP450 complex. Ligand topology was generated using SwissParam (CGenFF), and protein topology was prepared in GROMACS v2019.4. The complex was solvated in a dodecahedral TIP3P water box and neutralized. Energy minimization was performed using the steepest descent algorithm (5000 steps), followed by equilibration under NVT and NPT ensembles (10 ns each, 300 K) with positional restraints on ligand heavy atoms. A 10 ns production run was carried out using the leap-frog integrator. Structural stability was evaluated using root mean square deviation (RMSD) and conformational flexibility by Cα-root mean square fluctuation (RMSF), analyzed with standard GROMACS utilities.

Bio-efficacy assessment of linoleic acid against *H. armigera*

A diet overlay bioassay was used to assess the efficacy of linoleic acid against third instar *H. armigera* larvae. Linoleic acid (99% purity) was dissolved in 1% ethanol with Triton X-100 as a surfactant. Starved larvae (1 h) were individually placed in cell wells containing 2 mL of artificial diet treated with 200 µL of linoleic acid at seven concentrations (500–40,000 ppm). Two controls included: solvent (1% ethanol) and untreated diet. After air-drying, twelve larvae per concentration were tested in triplicate. Mortality was recorded after 72 h, with immobile larvae (failing to right themselves when flipped) scored as dead. LC_{50} values were estimated by probit analysis.

Data preparation for statistical Analysis

Plant proteomics data preparation

Proteomic datasets were generated from two resistant chickpea genotypes—one cultivated (ICCV506EB, R-1), one wild (IG73016, R-2)—and one susceptible genotype (ICC3137, S). Corresponding *H. armigera* larvae were designated Ha-R-1, Ha-R-2, and Ha-S. Plant protein quantification was performed by pairwise comparison of resistant (R-1, R-2) versus susceptible (S) genotypes. Differentially expressed proteins (DEPs) were classified as Resistant-Related Constitutive (RRC) or Resistant-Related Induced (RRI). RRC proteins were identified from resistant uninfested (RM) versus susceptible uninfested (SM) expression ratios (RRC = RM/SM), while RRI proteins were determined by normalizing resistant infested/uninfested (RP/RM) against susceptible infested/uninfested (SP/SM) ratios (RRI = [RP/RM]/[SP/SM]). Proteins with Log_2fold change ≥ 1.0 and false discovery rate (FDR) ≤ 0.05 were considered significant.

Insect proteomics data preparation

Midgut proteomes of insects fed on resistant genotypes (Ha-R-1, Ha-R-2) were compared with those fed on the susceptible genotype (Ha-S). Differentially expressed proteins (DEPs) were identified using Student's *t*-tests (Ha-R-1 vs

Ha-S; Ha-R-2 vs Ha-S), with fold change (FC) calculated as the abundance ratio between resistant-fed and susceptible-fed insects. DEPs with $Log_2FC \geq 1.0$ and FDR ≤ 0.05 were classified as *H. armigera* Resistance-Response Proteins (Ha-RRPs; upregulated in resistant-fed insects) or Susceptible-Response Proteins (Ha-SRPs; upregulated in susceptible-fed insects).

Statistical analysis

Pairwise Student's *t*-tests were applied to identify differentially expressed proteins (DEPs) under resistant versus susceptible conditions. In plants, comparisons included RP-1 vs RM-1, RP-1 vs SP, RM-1 vs SM, and SP vs SM for R-1, and RP-2 vs RM-2, RP-2 vs SP, and RM-2 vs SM for R-2. In insects, Ha-R-1 and Ha-R-2 were compared with Ha-S, which served as the common reference. Volcano plots were generated using SR Plot to visualize DEPs (log_2 fold change vs FDR), and Venn diagrams (Venn Diagram tool) were used to highlight overlapping and unique DEPs.

Multivariate analyses, including PCA and PLS-DA, were performed in MetaboAnalyst 6.0 to assess clustering and variation across groups. Group differences were evaluated using permutational multivariate analysis of variance (PERMANOVA). The PLS-DA model was evaluated using fivefold cross-validation and permutation testing (1000 iterations) to assess model robustness and potential overfitting. Functional annotation involved subcellular localization prediction and Gene Ontology (GO)-based classification of biological processes, molecular functions, and cellular components using UniProt and DAVID.

Results

Pod bioassay revealed resistance of chickpea genotypes against the *H. armigera*

Pod bioassays of chickpea genotypes, including cultivated genotypes and a CWR, revealed distinct resistance responses to *H. armigera*. The wild genotype IG73016 exhibited the lowest pod damage rating (PDR = 3) and larval weight gain (43.18%), indicating strong resistance. The resistant check ICCV506EB showed moderate resistance (PDR = 4.0; larval weight gain = 148.31%), whereas the susceptible cultivar ICC3137 displayed severe feeding damage (PDR = 8) and markedly higher larval weight gain (950.12%) (Fig. S2). Accordingly, *C. cuneatum* IG73016 was selected as the resistant wild genotype, with ICCV506EB and ICC3137 serving as resistant and susceptible cultivated checks, respectively. These representative genotypes were further used for proteomic profiling to dissect the molecular basis of chickpea defense against *H. armigera*.

Proteomic response in chickpea and its CWR against *H. armigera* infestation

Total proteins from resistant (cultivated and wild) and susceptible chickpea genotypes, under *H. armigera*-infested and uninfested conditions (24 h post-infestation), were analyzed using UPLC–MS/MS. A total of 485 proteins were identified using the chickpea UniProt database. The DEPs were defined as those supported by ≥ 2 unique peptides, Log_2fold change ≥ 1.0, and FDR ≤ 0.05, across four contrasts: RP/RM, RP/SP, RM/SM and SP/SM. Venn analysis revealed distinct and overlapping DEPs among treatments. In R-1, the SP/SM comparison contributed the most DEPs (325), with 240 unique proteins, followed by RM-1 vs SM (69), RP-1 vs SP (42) and RP-1 vs RM (41) (Fig. 1a). In R-2, RP-2 vs RM-2 showed the highest number of DEPs (353, including 52 unique), followed by SP vs SM (325), RM-2 vs SM (144) and RP-2 vs SP (136) (Fig. 1b).

Multivariate analysis confirmed clear treatment-dependent shifts. PCA revealed tight replicate clustering in all genotypes, with PC1 explaining 70–89% of variance and PC2 accounting for replicate-level differences. The wild genotype R-2 showed stronger separation (PC1 = 85.4%), while the susceptible genotype displayed the most pronounced contrast (PC1 = 89.3%). Separation between infested and uninfested samples was observed for each genotype (Fig. S3a–c), and PERMANOVA analysis supported treatment-associated differences based on permutation testing (999 permutations). PLS-DA further reinforced these trends, with well-separated, non-overlapping clusters across genotypes, highlighting strong and genotype-specific proteomic remodeling upon insect infestation (Fig.S3d–f). Model evaluation indicated high goodness-of-fit ($R^2 \approx 0.99$) and predictive ability ($Q^2 \approx 0.96$), and fivefold cross-validation with permutation testing (1000 iterations) indicated stable model performance with low risk of overfitting (Fig.S3 g-i).

Functional classification of identified proteins based on GO annotation for chickpea

GO annotation of the 485 identified proteins revealed genotype-specific enrichment patterns across biological processes (BP), cellular components (CC), and molecular functions (MF). In R-1, enriched BP included de novo UMP and pyrimidine nucleobase biosynthesis, along with glycolysis. CC terms were predominantly associated with the nucleus and cytoskeleton, while MF enrichment highlighted orotate phosphoribosyl transferase, orotidine-5′-phosphate decarboxylase, and ribonucleoside binding activities (Fig. 2a). In contrast, R-2 showed enrichment in BP related to RNA

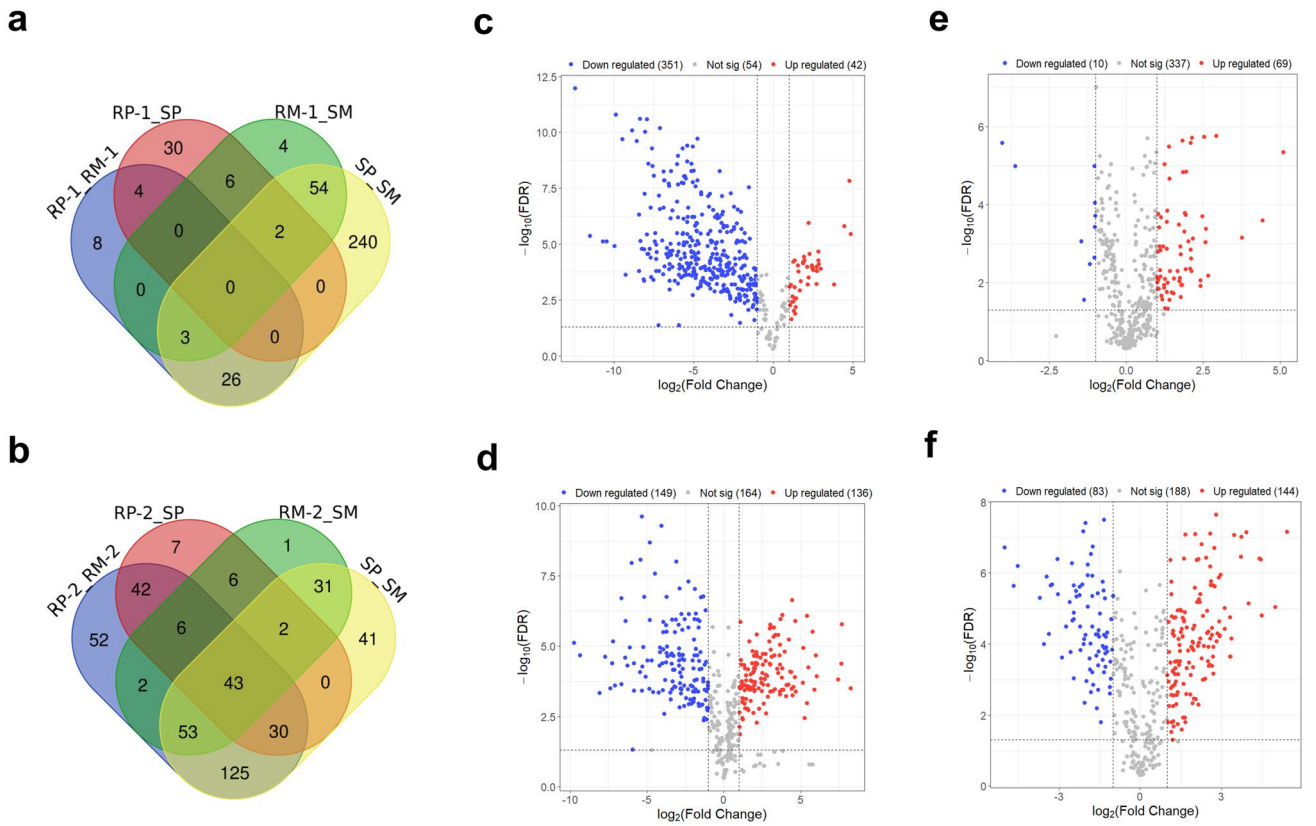

Fig. 1 Venn diagrams illustrate the overlap and unique sets of differentially expressed proteins (DEPs) identified in two resistant chickpea genotypes—(**a**) R-1 (ICCV506EB) and (b) R-2 (IG73016)—in comparison with the susceptible genotype S (ICC3137). Comparisons include RP/RM, RP/SP, RM/SM, and SP/SM. *RP* resistant infested, *RM* resistant uninfested, *SP* susceptible infested, *SM Susceptible Uninfested*. Volcano plots display significantly accumulated proteins (FDR < 0.05, $Log_2FC > 1$) for the resistant genotypes: **c** RP-1 vs SP and **d** RP-2 vs SP under infected conditions, and **e** RM-1 vs SM and **f** RM-2 vs SM under Uninfested conditions. Red and blue dots indicate upregulated and downregulated proteins, respectively

polymerase II-mediated transcription, chromatin remodeling, mitotic DNA replication initiation, and 1,3-β-D-glucan biosynthesis. CC terms were enriched for the DNA polymerase III complex, transcription elongation factor complex, and 1,3-β-D-glucan synthase complex, while MF analysis revealed strong enrichment of orotate phosphoribosyl transferase, orotidine-5′-phosphate decarboxylase, and 1,3-β-D-glucan synthase activities (Fig. 2b).

Differential protein expression in resistant genotypes compared to the susceptible genotype

Comparative analysis of resistant versus susceptible genotypes revealed distinct expression patterns of differentially expressed proteins (DEPs) under Infested (RP vs SP) and Uninfested (RM vs SM) conditions. Under infested condition, R-1 (RP-1: ↑ 42, ↓351) showed predominantly downregulated proteins, suggesting suppression of stress-related pathways, whereas R-2 (RP-2: ↑136, ↓149) exhibited a more balanced regulation, indicative of dynamic defense activation (Fig. 1c, d). Under constitutive conditions, both R-1 (RM-1: ↑69, ↓10) and R-2 (RM-2: ↑144, ↓83) showed strong upregulation, reflecting enhanced basal defense capacity (Fig. 1e, f).

Resistance-related constitutive proteins (RRC)

Resistance-related constitutive (RRC) proteins were identified by comparing resistant genotypes with the susceptible genotype under uninfested condition at 24 hpi. A total of 69 RRC-1 proteins were detected in R-1 and 144 RRC-2 proteins in R-2 (Tables S2 and S4). Among the prominent proteins with significant fold changes were those related to the plant cell wall, including galactinol-sucrose galactosyltransferase (3.75 log_2FC), cellulose synthase-like protein D3 (2.13 log_2 FC), β-glucosidase 40-like (2.09 log_2FC), glucomannan 4-β-mannosyltransferase 9-like (1.20 log_2FC), 1,3-β-glucan synthase (1.42 log_2FC), and non-reducing end α-L-arabinofuranosidase (1.13 log_2FC). Several receptor proteins showed notable upregulation, such as

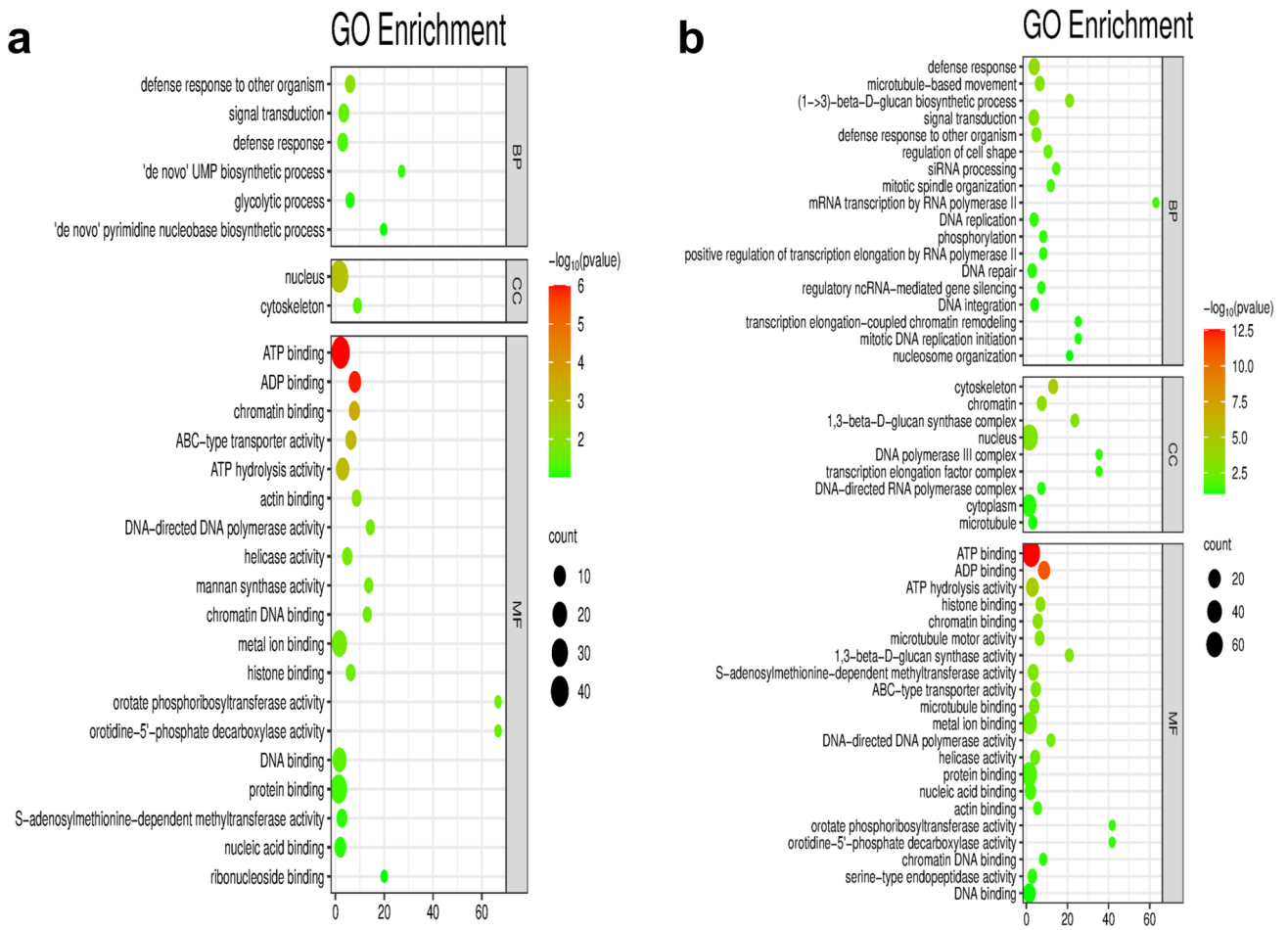

Fig. 2 Gene Ontology enrichment analysis of differentially expressed proteins identified in two resistant chickpea genotypes—ICCV506EB (R-1) and IG73016 (R-2)—compared to the susceptible genotype ICC3137 (S). a and b represent the GO classification results for R-1 and R-2, respectively. Proteins were categorized under three major GO domains: BP biological process, CC cellular component, MF molecular function. The size of each circle indicates the number of proteins associated with each GO term, and the color scale represents the statistical significance (p-value) of enrichment, with darker colors indicating higher significance

wall-associated receptor kinase 2-like (2.42 log_2FC), receptor-like serine/threonine-protein kinase ALE2 isoform X1 (2.52 log_2FC), non-specific serine/threonine protein kinase (2.10 log_2FC), and receptor-like protein kinase FERONIA (1.62 log_2FC). ROS-related proteins were also elevated, including heat shock protein (2.47 log_2FC), chaperone protein ClpC (1.00 log_2FC), and acylaminoacyl-peptidase (1.94 log_2FC).

Transcription factors demonstrating increased abundance comprised of WRKY transcription factor 40 (1.35 log_2FC), zinc finger CCCH domain-containing protein 55 isoform X1 (1.93 log_2FC), zinc finger protein 1 (2.00 log_2FC), transcription elongation factor SPT6-like (2.22 log_2FC), and HECT-type E3 ubiquitin transferase (2.27 log_2FC). Lastly, fatty acid pathway proteins such as 1-phosphatidylinositol-3-phosphate 5-kinase (1.80 log_2FC), 1-phosphatidylinositol 4-kinase (1.54 log_2FC), phosphatidylinositol/phosphatidylcholine transfer protein SFH12-like isoform X2 (1.00 log_2FC), and phospholipase D (0.08 log_2FC), were among those notably upregulated.

Resistance-related induced proteins (RRI)

Resistance-related induced (RRI) proteins were identified by comparing resistant and susceptible genotypes at 24 hpi, yielding 28 RRI-1 proteins in R-1 and 126 RRI-2 proteins in R-2 (Tables S3 and S5). Among these, cell wall-related proteins such as cellulose synthase interactive protein 1 isoform X2 (6.11 log_2FC), 1,3-β-glucan synthase (5.17 log_2FC), β-glucosidase 40-like (3.69 log_2FC), cellulose synthase-like protein B4 isoform X1 (2.96 log_2FC), and purple acid phosphatase (3.36 log_2FC) were predominantly upregulated.

Receptor proteins, including receptor kinase-like protein Xa21 (3.41 log_2FC), serine/threonine-protein kinase

PRP4 homolog (5.42 log_2FC), mitogen-activated protein kinase (3.90 log_2FC), and non-specific serine/threonine protein kinase (2.58 log_2FC), showed increased expression. Even the ROS-related protein viz., ROS1-like protein (1.42 log_2FC) was also induced.

Phytohormone-related proteins like gibberellin 2-β-dioxygenase 2 (3.70 log_2FC), 1-aminocyclopropane-1-carboxylate synthase (1.00 log_2FC), cytochrome P450 711A1 isoform X2 (3.09 log_2FC) were elevated. Key transcription factors included WRKY transcription factor 40 (3.12 log_2FC) and transcriptional elongation regulator MINIYO isoform X2 (1.02 log_2FC). Fatty acid metabolism pathway-related proteins, such as lipase (3.40 log_2FC), phosphatidylinositol 4-phosphate 5-kinase (3.08 log_2FC), lysophospholipid acyltransferase LPEAT2 (2.81 log_2FC), phospholipase D (1.88 log_2FC), and Lipoxygenase-LOX (1.02 log_2FC) (LOX was uniquely identified using the soybean UniProt database), showed enhanced abundance. Even the terpenoid pathway protein—terpene synthase (1.00 log_2FC), was uniquely identified using the soybean UniProt database.

Comparative gut proteomics of *H. armigera* fed on chickpea and its CWR.

Insect midgut proteins from *H. armigera* larvae fed on resistant (Ha-R-1, Ha-R-2) and susceptible (Ha-S) chickpea genotypes were analyzed by UPLC—MS/MS, yielding 674 proteins (UniProt database). Comparative analysis identified 155 proteins in Ha-RRP-1, 120 in Ha-SRP-1, 189 in Ha-RRP-2, and 116 in Ha-SRP-2 at 24 hpi. Venn diagram analysis revealed 120 proteins common to resistant-fed larvae, with Ha-RRP-1 and Ha-RRP-2 showing 35 and 68 unique proteins, respectively (Fig. 3a). In susceptible-fed larvae, 61 proteins were shared, with 59 unique to Ha-SRP-2 and 54 to Ha-SRP-1 (Fig. 3b).

Multivariate analysis confirmed clear segregation of midgut proteomes. PCA showed distinct clustering, with PC1 (60.2%) and PC2 (39.2%) capturing > 99% of variance. Ha-S clustered separately from resistant-fed groups, while Ha-R-1 and Ha-R-2 formed distinct clusters with minimal replicate variability (Fig. 3c). PERMANOVA analysis confirmed that the differences among groups based on permutation testing (999 permutations). PLS-DA reinforced these findings, with

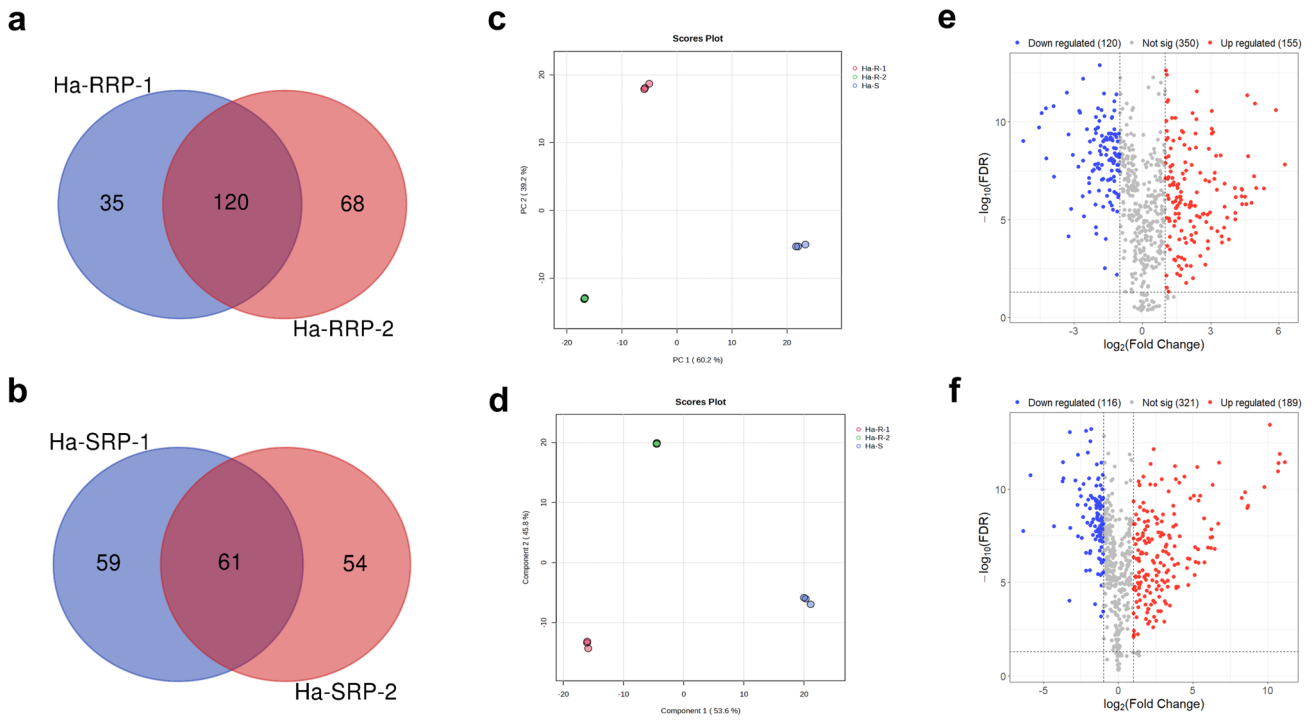

Fig. 3 Venn diagrams and multivariate analyses of differentially expressed proteins (DEPs) in *H. armigera* larvae fed on resistant and susceptible chickpea genotypes. **a** Overlap and unique sets of Resistance-Response Proteins (RRPs) identified in insects fed on resistant genotypes (Ha-R-1, Ha-R-2) compared with susceptible-fed insects (Ha-S). **b** Overlap and unique sets of Susceptible-Response Proteins (SRPs) identified in susceptible-fed insects relative to resistant-fed insects. Proteins were considered significant based on Log_2 fold change ≥ 1.0 and FDR ≤ 0.05, highlighting both common and genotype-specific midgut responses. **c** PCA and **d** PLS-DA plots showing clustering and group separation of midgut proteomes in insects fed on resistant (Ha-R-1, Ha-R-2) and susceptible (Ha-S) genotypes. (**e–f**) Volcano plots depicting DEPs between resistant- and susceptible-fed insects: **e** Ha-R-1 vs Ha-S and **f** Ha-R-2 vs Ha-S. Red and blue dots represent significantly upregulated and downregulated proteins, respectively

Component 1 (53.6%) and Component 2 (45.8%) explaining > 99% of variance. Resistant-fed groups clustered apart from Ha-S, with Ha-R-1 and Ha-R-2 forming well-defined, genotype-specific clusters (Fig. 3d). Model evaluation indicated high goodness-of-fit ($R^2 = 0.94–0.999$) and predictive ability ($Q^2 = 0.87–0.999$), and fivefold cross-validation with permutation testing (1000 iterations) suggested stable model performance with low risk of overfitting (Fig. S3j).

Functional classification of identified proteins based on GO annotation for *H. armigera*

GO enrichment analysis of DEPs from resistant-fed larvae (Ha-R-1, Ha-R-2) versus susceptible-fed larvae (Ha-S) revealed distinct functional profiles across all GO domains.

In Ha-R-1, enriched Biological Process (BP) terms included *protein phosphorylation* (GO:0006468), *DNA biosynthetic process* (GO:0071897), *cell migration* (GO:0016477), *DNA repair* (GO:0006281), *cell surface receptor protein tyrosine kinase signaling pathway* (GO:0007169), and *cell division* (GO:0051301). Within the Cellular Component (CC) domain, the most enriched terms were *cytoplasm* (GO:0005737), *plasma membrane* (GO:0005886), *cytoskeleton* (GO:0005856), and *chromosome* (GO:0005694). In the Molecular Function (MF) category, significant enrichment was observed for *ATP binding* (GO:0005524), *protein binding* (GO:0005515), *metal ion binding* (GO:0046872), *ATP hydrolysis activity* (GO:0016887), and *mRNA binding* (GO:0003729). Several kinase-related activities, including *histone H3S57 kinase activity* (GO:0140855), *DNA-dependent protein kinase activity* (GO:0004677), and *AMP-activated protein kinase activity* (GO:0004679), were also enriched, alongside transporter functions such as *ABC-type transporter activity* (GO:0140359) and *lipid transporter activity* (GO:0005319) (Fig. 4a).

In Ha-R-2, the BP category showed enrichment for *protein phosphorylation* (GO:0006468), *DNA biosynthetic process* (GO:0071897), *cell migration* (GO:0016477), *monatomic ion transport* (GO:0006811), and *homophilic cell adhesion* via *plasma membrane adhesion molecules* (GO:0007156). Enriched CC terms included *nucleus* (GO:0005634), *cytoplasm* (GO:0005737), *plasma membrane* (GO:0005886), and *cytoskeleton* (GO:0005856). In the MF category, the top enriched terms were *ATP binding* (GO:0005524), *protein binding* (GO:0005515), *metal ion binding* (GO:0046872), *ATP hydrolysis activity* (GO:0016887), and *mRNA binding* (GO:0003729) (Fig. 4b).

Differential gut protein expression in *H. armigera* fed on resistant vs. susceptible genotypes.

The comparison of DEPs between resistant-fed (Ha-R-1, Ha-R-2) and susceptible-fed larvae (Ha-S) revealed distinct

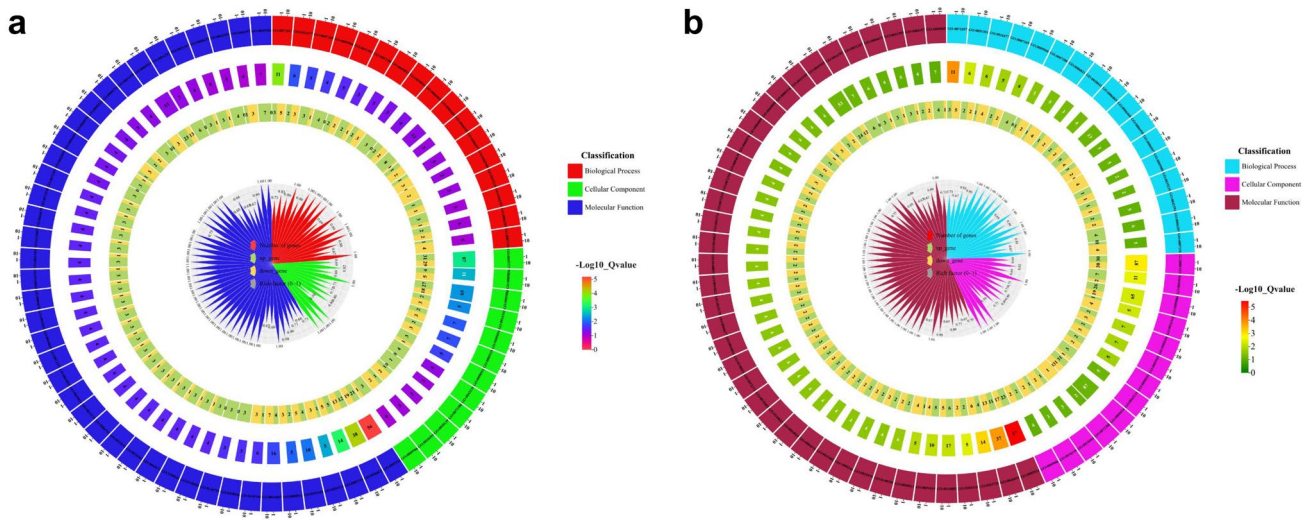

Fig. 4 Gene Ontology (GO) enrichment analysis of differentially expressed proteins (DEPs) in the midgut of *H. armigera* larvae fed on resistant versus susceptible chickpea genotypes. **a** GOCircle plot showing functional classification of DEPs in larvae fed on the resistant genotype Ha-R-1 compared with the susceptible genotype Ha-S. **b** GOCircle plot showing functional classification of DEPs in larvae fed on the resistant genotype Ha-R-2 compared with the susceptible genotype Ha-S. In each plot, GO terms are grouped into Biological Process, Cellular Component, and Molecular Function categories, as indicated by distinct colors. The inner radial bars represent the number of genes associated with each term, separated into upregulated and downregulated proteins, with segments containing both shown as a combination of the colors. The outermost ring lists GO term names, the middle ring shows gene counts, and the inner heatmap ring depicts enrichment significance as $-\log_{10}$(Q-value), with higher values indicating greater significance. The central radial scale also displays the rich factor (0–1) for each GO term

regulatory trends. Ha-R-1/Ha-S showed a strong upregulation bias (↑155, ↓120), indicative of an activation-driven proteomic response, whereas Ha-R-2/Ha-S also displayed a pronounced upregulation trend (↑189, ↓116), suggesting an intensified activation and reprogramming of the proteome (Fig. 3e, f).

***H. armigera* Resistance Response Proteins (Ha-RRPs)** Key Ha-RRPs included a variety of functional categories (Table S6). Digestive enzymes such as aminopeptidase (3.74 log_2FC), salivary protein (1.00 log_2FC), metalloendopeptidase (1.20 log_2FC), and peptidase S1 domain-containing protein (3.44 log_2FC) were notably upregulated. Among receptors, proteins like: MAP4K (2.97 log_2FC), receptor serine/threonine kinase (2.45 log_2FC), GPCR family 1 protein (1.87 log_2FC), nicotinic acetylcholine receptor α3 (1.70 log_2FC), NMDA receptor subunit 3A (1.21 log_2FC), tyrosine-protein kinase Wsck (2.39 log_2FC), EGF-like protein (3.08 log_2FC) showed increased expression. Proteins involved in ROS management, such as peroxidase (2.19 log_2FC), HSP22 (4.69 log_2FC), HSP70 cognate 5 (2.92 log_2FC), NADP-dependent oxidoreductase (4.61 log_2FC), apoptosis inhibitor 5 (1.11 log_2FC), were significantly elevated. Detoxification enzymes including cytochrome P450 (2.01 log_2FC), UDP-glycosyltransferase (5.73 log_2FC), monooxygenase (1.00 log_2FC), aldehyde reductase 10 (1.00 log_2FC), carboxylic ester hydrolase (3.62 log_2FC), γ-glutamylcyclotransferase (3.64 log_2FC), carboxylesterase type B protein (1.20 log_2FC) were also upregulated. Transcription factors, viz., GTF3C3 (2.97 log_2FC), RING-type protein (1.63 log_2FC), C2H2-type protein (3.49 log_2FC), RRM protein (3.86 log_2FC), CCHC-type protein (5.87 log_2FC), were enhanced.

Transporters, including SEC23 (1.97 log_2FC), ion transport protein (3.19 log_2FC), ABC transporter (2.47 log_2FC), MFS protein (4.64 log_2FC), potassium channel protein (1.35 log_2FC), and V-type proton ATPase (1.88 log_2FC), were also more abundant. Additionally, proteins associated with midgut integrity, such as adenylate kinase (4.54 log_2FC), cadherin-domain protein (1.53 log_2FC), were significantly expressed.

H. armigera-Susceptible Response Proteins (Ha-SRPs)

Representative Ha-SRPs with notable fold changes included (Table S7): digestive enzymes such as cathepsin L-like protease (1.00 log_2FC), aminopeptidase (2.14 log_2FC), malic enzyme (1.32 log_2FC). Among receptors, the NMDA receptor subunit 1 (2.47 log_2FC), protein kinase domain protein (2.06 log_2FC), tyrosine-protein kinase receptor (2.16 log_2FC). Proteins involved in ROS management, including HSP70 (3.25 log_2FC), superoxide dismutase (1.11 log_2FC), HSP19.5 (1.00 log_2FC), and J domain-containing protein (2.47 log_2FC), was also elevated. Detoxification enzymes such as cytochrome P450 (1.42 log_2FC), UDP-glucuronosyltransferase (1.42 log_2FC), monooxygenase (1.16 log_2FC) were upregulated. Transcription factors, including the TFIIC 90 kDa subunit (1.00 log_2FC), the PWI domain protein (5.25 log_2FC), and the C2H2-type protein (1.77 log_2FC), exhibited increased abundance. Transport-related proteins, such as ABC transporter (1.95 log_2FC), signal recognition particle 9 kDa protein (1.19 log_2FC), MFS protein (2.57 log_2FC), and sodium channel protein (2.52 log_2FC), were also more abundant. Additionally, the cadherin-domain protein (1.69 log_2FC), linked to Midgut integrity was upregulated.

Validation of plant protein expression

Expression of twelve defense-related genes was validated by qRT-PCR, spanning cell wall biosynthesis, receptor kinases, calcium signaling, R proteins, transcription factors, phytohormone pathways, fatty acid metabolism, and terpene biosynthesis. Consistent with proteomic profiles, several genes showed significant upregulation ($p < 0.05$) in resistant versus susceptible genotypes, including *CELLULOSE SYNTHASE INTERACTIVE 1* (2.3–4.68 FC), *1,3-β-glucan synthase* (2.76–3.09 FC), receptor-like serine/threonine-protein kinase (2.06–3.14 FC), calcium-transporting ATPase (2.46–3.23 FC), CC-NBS-LRR protein (2.03–2.83 FC), *GA 2-β-dioxygenase 2* (3.62–4.60 FC), *ABA 8'-hydroxylase 4* (2.70–5.47 FC), lipase (2.68–4.81 FC), phosphatidylinositol 4-phosphate 5-kinase (3.49–4.98 FC), terpene synthase (2.69–3.22 FC), *WRKY40* (3.49–4.64 FC), and ethylene receptor (2.83–8.96 FC). These results confirm proteomic trends and underscore genotype-specific expression signatures underlying resistance (Fig. 5).

Molecular docking and dynamics confirm stable binding of linoleic acid to CYP450 in *H. armigera*

Herbivore attack induces phospholipase-mediated release of linoleic (18:2) and linolenic (18:3) acids, with linolenic acid driving jasmonic acid (JA) synthesis via the octadecanoid pathway (Qi et al. 2011; Nishizato et al. 2025; Hunter et al. 2025). As a central defense signal, JA coordinates diverse anti-herbivore responses, thereby linking fatty acid turnover to plant resistance (Vatanparast et al. 2020; Hunter et al. 2025). Based on this, we selected linoleic acid as the ligand for initial molecular docking studies with key insect digestive enzymes (Aminopeptidase, Peptidase) and detoxification enzymes (Cytochrome P450, UDP-glycosyltransferase, Carboxylesterase, Aldehyde reductase). Among these, the best docking results were obtained with CYP450. In *H. armigera*, the CYP450 model quality was confirmed through Ramachandran analysis, showing 92.5%

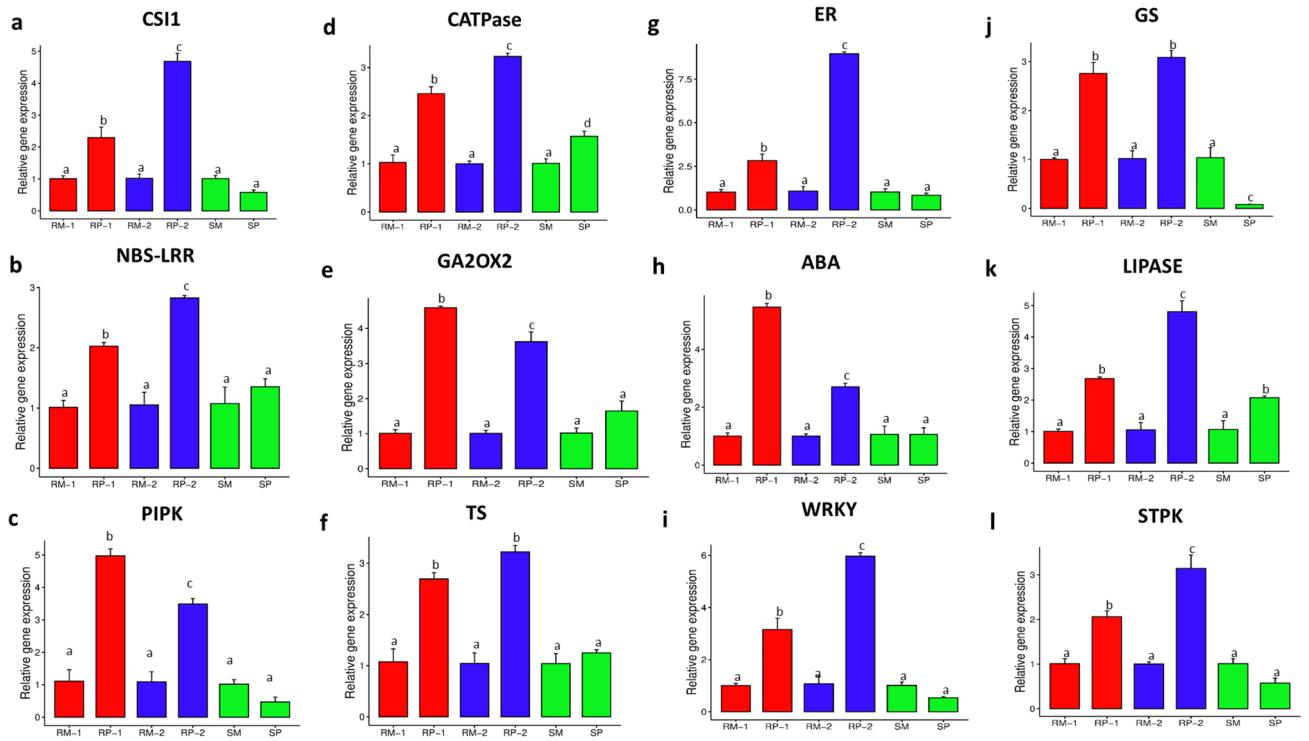

Fig. 5 Relative expression of candidate genes (**a–l**) in resistant and susceptible chickpea genotypes. Quantitative real-time PCR (RT-qPCR) analysis showing transcript abundance of the indicated genes under uninfested and infested conditions. RM-1 and RP-1 represent the cultivated resistant check ICCV 506 EB (uninfested and infested, respectively), RM-2 and RP-2 correspond to the wild resistant genotype IG 73016 (uninfested and infested, respectively), and SM and SP denote the cultivated susceptible check ICC 3137 (uninfested and infested, respectively). Data represent mean ± SE from three biological replicates. Different letters above the bars indicate statistically significant differences ($p < 0.05$, one-way ANOVA followed by post hoc test)

of residues in most favoured and 7.1% in allowed regions, validating its suitability for docking (Fig. S4). Docking studies revealed strong binding of plant linoleic acid to midgut CYP450 of *H. armigera* (–7.2 kcal/mol, AutoDock Vina). Structural visualization (BIOVIA Discovery Studio) indicated multiple stabilizing interactions, including hydrogen bonds (ASN116, PHE113, PHE119), hydrophobic contacts (LEU324, ALA328, PHE325, ALA191, ILE187), van der Waals forces (ILE475, VAL327, GLY329), and aromatic interactions (PHE113, PHE118, PHE479) (Fig. 6a–c). Collectively, these results demonstrate a stable and favorable interaction of linoleic acid with CYP450.

Structural stability and dynamic behavior of the CYP450–linoleic acid complex

All-atom MD simulations (10 ns, GROMACS) were conducted to assess the stability of the CYP450–linoleic acid complex. Backbone RMSD analysis showed rapid equilibration within 1 ns, with values stabilized between 0.20–0.28 nm, indicating structural stability without significant drift (Fig. 6d). RMSF analysis revealed low residue-level fluctuations (< 0.1 nm), with reduced flexibility in the active-site region, confirming a rigid and stable binding pocket (Fig. 6e). These results demonstrate that linoleic acid remained stably accommodated within the CYP450 active site, maintaining overall structural integrity of the complex.

Probit analysis of linoleic acid bioassay

The insecticidal potential of linoleic acid against third instar *H. armigera* larvae was evaluated using the diet overlay method. Probit analysis of three-day mortality data estimated an LC_{50} of 15,083.845 ppm (95% CL: 0.889–1.536) and an LC_{95} of 342,712.243 ppm (Fig. S5). The dose–response slope (1.121 ± 0.165) and χ^2 value (7.397) indicated a moderate yet reliable fit to the probit model. These results demonstrate that linoleic acid exerts toxic effects on *H. armigera* larvae.

These results indicate that LA exhibits measurable larval toxicity under the tested conditions. However, the bioassay evaluated mortality only, and no direct measurements of physiological or immune parameters were conducted; therefore, any proposed effects beyond general toxicity require further experimental validation.

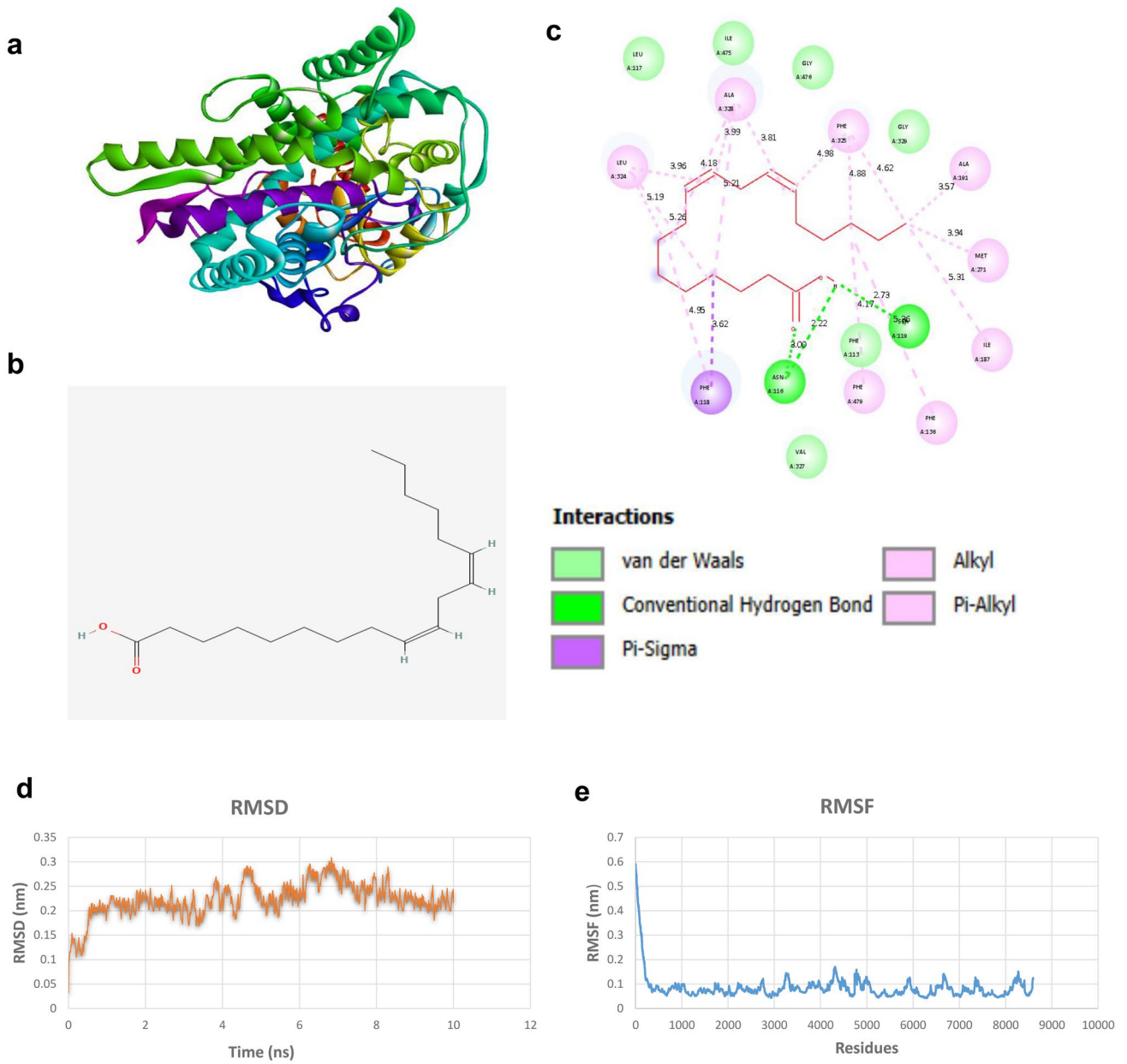

Fig. 6 Molecular docking and dynamics of insect cytochrome P450 (CYP450) with linoleic acid (LA). **a** Predicted 3D structure of insect CYP450 used for docking. **b** 2D structure of linoleic acid (LA; CAS Registry Number 60–33-3) used as the ligand. **c** Docking interaction profile of CYP450 with LA. Molecular dynamics (MD) simulations of the CYP450–LA complex: **d** root mean square deviation (RMSD) plot showing structural stability of the complex over a 10 ns trajectory, and **e** root mean square fluctuation (RMSF) plot depicting residue-wise flexibility during the simulation

Discussion

Plants are constantly being challenged by insect herbivores that threaten their growth, productivity, and yield. To counter these challenges, they have evolved a wide array of defense strategies, including the production of secondary metabolites and defense proteins that deter feeding, impair insect development, or exert direct toxic effects on herbivores (Gatehouse 2002; Chen 2008; Wu and Baldwin 2010; Ali et al. 2024). However, many crop species have experienced genetic erosion during domestication and large-scale cultivation, loosing crucial adaptive traits against biotic stresses. In contrast, crop wild relatives remain an invaluable reservoir of genetic diversity, retaining traits for resilience against environmental and biotic stresses (Zhang et al. 2019a; Singh et al. 2021). In chickpea, the narrow genetic base of cultivated varieties emphasizes the importance of exploiting wild *Cicer* species, which have co-evolved

under constant herbivory and exhibit robust direct defense mechanisms against *H. armigera* (Golla et al. 2018b, 2020). This study utilized comparative proteomics to unravel the molecular basis of chickpea resistance to *H. armigera*. By capturing the dynamic interaction changes in host and insect proteomes, the analysis sheds light on the proteolytic "tug-of-war" between resistant chickpea genotypes deploying defense proteins and inhibitors. Though the insect attempts effectively, but fails to mount adaptive counter-responses, leading to mortality.

Molecular Arms Race: Chickpea–*H. armigera* Interactions

The interaction between chickpea and *H. armigera* exemplifies a classical molecular arms race, wherein the host plant deploys a series of defense mechanisms to restrict insect feeding. Conversely, the insect evolves adaptive counterstrategies to sustain its growth and survival but fails to survive when fed on resistant wild chickpea genotypes.

Resistance-Related Proteins in Chickpea–H. armigera Interaction: Upon *H. armigera* infestation, resistant chickpea activates a diverse array of defense responses, including the induction of receptor kinases, phytohormones, transcription factors, and proteins related to secondary biosynthetic pathways, that collectively impair insect digestion and disrupt midgut physiology (Napoleão et al. 2019). Upon herbivore attack, plants detect damage- and herbivore-associated molecular patterns (DAMPs and HAMPs) through pattern recognition receptors (PRRs), including receptor-like kinases (RLKs), initiating early defense signaling (Erb and Reymond 2019). In this study, resistant chickpea genotypes exhibited upregulation of leucine-rich repeat RLKs, receptor-like serine/threonine kinases, stress-induced RLK2, and Xa21-like kinases following *H. armigera* infestation. Comparable findings in rice (*OsLRR-RLK1*) and tea (*CsLRR-RLK44/239*) demonstrate that herbivore-induced RLKs activate MAPK cascades and downstream defenses (Hu et al. 2018; Jiang et al. 2025). MAPKs were consistently upregulated in resistant chickpea genotypes, indicating their role as early amplifiers of defense responses. MAPK cascades, through sequential phosphorylation events (MAPKKK → MAPKK → MAPK), activate specific transcription factors, hormone signaling (JA, SA), and defense-related genes (Rodriguez et al. 2010; Pitzschke 2015). In the present study, activation of the JA pathway is inferred based on the differential abundance of JA biosynthesis- and signaling-related proteins identified in the proteomic analysis. Direct quantification of JA or its derivatives using targeted hormone profiling will be required to confirm JA accumulation under herbivore infestation. Previous reports in tomato, tobacco, and rice support MAPK-mediated regulation of JA/SA signaling in herbivore-induced resistance (Kandoth et al. 2007; Wu et al. 2007; Wang et al. 2013).

The coordinated induction of RLKs and MAPKs in resistant chickpea genotypes underscores their critical role in early herbivore recognition and signal amplification. Acting as molecular switches, these receptors integrate herbivore perception with MAPK cascades and hormonal networks, thereby enabling rapid transcriptional reprogramming and enhancing resistance against *H. armigera*.

Transcription factors (TFs) are pivotal regulators of plant defense, orchestrating transcriptional reprogramming in response to herbivore attack. Proteomic analysis in this study revealed significant upregulation of WRKY40, MYB-type TFs, zinc finger proteins (C2H2- and PHD-type), and E3 ubiquitin ligases (RING- and HECT-type) in resistant chickpea genotypes following *H. armigera* infestation, highlighting their vital role in activating defense pathways. WRKY TFs, often acting downstream of MAPK cascades, were strongly induced, with WRKY40 showing a consistent role in herbivore resistance, as previously demonstrated in Arabidopsis, tobacco, and rice (Schweizer et al. 2013; Chujo et al. 2014; Li et al. 2015; Yao et al. 2020). MYB TFs are known to regulate both chemical and structural defenses, including cell wall modification and callose deposition (Vos et al. 2006; Zhai et al. 2017), suggesting similar roles in chickpea. Zinc finger proteins, particularly C2H2- and PHD-types, have been widely implicated in transcriptional reprogramming during herbivory across species (Lawrence et al. 2018; Zhang et al. 2024), and their induction points to broad-spectrum defense roles. Additionally, RING- and HECT-type E3 ubiquitin ligases likely contribute to immune signaling through protein turnover, consistent with reports of RING-type ligases regulating JA signaling by modulating WRKY stability (Ali et al. 2019; Kawaguchi et al. 2023).

Proteomic analysis revealed the upregulation of several phytohormone-related proteins in resistant chickpea genotypes following *H. armigera* infestation, including 1-aminocyclopropane-1-carboxylate synthase (ACS), gibberellin 2-beta-dioxygenase 2 (GA2ox2), auxin response factors (ARFs), and abscisic acid 8′-hydroxylase 4, suggesting a complex interplay of hormonal pathways in defense regulation. Among these, ACS is a key enzyme in ethylene biosynthesis, and its induction highlights the central role of ethylene (ET) in insect-induced defense. ET functions both independently and synergistically with JA pathway to activate downstream signaling, regulate secondary metabolite production, and reinforce structural barriers such as callose deposition and cell wall thickening (Arimura et al. 2000; Schmelz et al. 2003; Varsani et al. 2019). The observed induction of 1,3-β-D-glucan synthase further supports ET-mediated reinforcement of physical defenses against herbivory.

In parallel, GA2ox2 upregulation suggests suppressing gibberellin activity, consistent with growth–defense trade-offs reported under herbivore pressure (Pandey et al. 2017; Li et al. 2022). Similarly, induction of ARFs points to auxin signaling as an early modulator of herbivore responses, often acting in concert with JA to regulate defense-related genes (Machado et al. 2016; Bhattacharjee et al. 2020). Resistant chickpea genotypes undergo hormone-mediated reprogramming, where oxylipin, ethylene, gibberellin, and auxin signaling converge to suppress growth and reinforce defense. The coordinated induction of transcription factors and phytohormones links early perception and MAPK signaling to the activation of secondary metabolic pathways, enabling an effective response against *H. armigera*. Similarly, significant upregulation of defense genes in wild pigeonpea (*C. scarabaeoides*) highlights robust defense pathway activation, accompanied by shifts in transcription factors, phytohormones, and calcium signaling (Meshram et al. 2025).

Proteomic analysis revealed the upregulation of several fatty acid pathway-related proteins in resistant chickpea genotypes following *H. armigera* infestation, including lipoxygenase (LOX), lipase, phospholipase D (PLD), lysophospholipid acyltransferase, phosphatidylinositol 4-phosphate 5-kinase (PIP5K), 1-phosphatidylinositol-3-phosphate 5-kinase (PI3P5K), AB hydrolase-1, enoyl reductase (ER), and phospholipid/glycerol acyltransferase domain-containing proteins. This coordinated induction suggests a pivotal role of lipid metabolism and signaling in defense responses. Lipases and PLDs are particularly important, as they liberate polyunsaturated fatty acids (PUFAs) and generate phosphatidic acid (PA), key precursors and second messengers in JA signaling, a central pathway in herbivore defense (Wang et al. 2000; Bonaventure et al. 2011). Similar associations have been reported in *C. scarabaeoides*, where lipase induction correlated with defense lipid production (Ngugi-Dawit et al. 2021). The observed upregulation of PIP5K and PI3P5K further underscores the role of phosphoinositide signaling in stress adaptation, as these kinases regulate $PI(4,5)P_2$ and $PI(3,5)P_2$ pools that influence membrane trafficking, cytoskeletal remodeling, and defense signaling (Heilmann 2016; Kuroda et al. 2021). These results suggest that resistant chickpea genotypes mobilize lipid-derived signaling cascades that are consistent with activation of JA-mediated defenses and strengthen resilience against *H. armigera*. Together, these multilayered defenses create a hostile biochemical environment that affects larval feeding efficiency and survival.

The current findings reflect an early defense response observed at 24 h post-infestation, and comprehensive time-course studies will be necessary to elucidate the full temporal progression of resistance mechanisms.

Proteolytic Countermeasures in H. armigera Midgut: In response to resistant chickpea genotypes, *H. armigera* remodels its midgut proteome through the upregulation of detoxification enzymes, including cytochrome P450 monooxygenases (P450s), glutathione-S-transferases (GSTs), carboxylesterases (CarEs), aldo–keto reductases, and ATP-binding cassette (ABC) transporters. These enzymes metabolize plant-derived allelochemicals but impose a significant metabolic cost, as their synthesis diverts resources from growth and development (Castañeda et al. 2009; Mulla and Tamhane 2023). The pod bioassay results corroborate this trade-off, with larvae feeding on resistant genotypes exhibiting reduced weight gain and delayed development despite an active detoxification response. Similar detoxification costs have been documented in *H. zea*, *Spodoptera* spp., and aphids under chemically defended diets (Yu and Hsu 1993; Francis et al. 2005; Chen et al. 2023).

The midgut epithelium is the critical interface where these defenses and counter-defenses are enacted. Resistant chickpea genotypes expose *H. armigera* larvae to secondary metabolites that impair digestive enzyme activity, affect nutrient uptake, and disrupt metabolic balance (Golla et al. 2018a; Chamani et al. 2025). Consequently, nutrient assimilation is inefficient, resulting in slower growth and higher mortality. In contrast, larvae feeding on susceptible genotypes experience minimal biochemical stress, as indicated by low to moderate levels of digestive enzymes such as aminopeptidases and peptidase S1 domain proteins, and therefore do not mount a compensatory enzymatic response due to the presence of fewer antinutritional barriers (Golla et al. 2018a).

These findings highlight the proteolytic tug-of-war at the plant–insect interface, where chickpea defense proteins suppress digestion and force larvae to energetically activate the detoxification strategies. This trade-off reduces herbivore fitness and underscores the potential of targeting insect proteases and detoxification pathways for breeding durable resistance in chickpea.

Oxidative stress–mediated trade-offs

Proteomic analysis revealed that *H. armigera* larvae feeding on resistant chickpea genotypes experience severe physiological stress, including oxidative imbalance, digestive impairment, and endocrine disruption, ultimately reducing fitness and survival. Elevated oxidative stress was evident from increased NAD(P)H oxidase activity and limited induction of antioxidant enzymes such as superoxide dismutase (SOD), resulting in redox imbalance and cellular damage (Ha et al. 2009; Jones et al. 2013; Lomate et al. 2015). Concurrent upregulation of heat shock proteins (HSP22.0, HSP70) indicated proteotoxic stress triggered by prolonged ROS accumulation (King and MacRae 2015). In contrast, larvae on susceptible genotypes displayed balanced

antioxidant activity (SOD, thioredoxin, HSP70), maintaining redox homeostasis.

Oxidative damage in the midgut epithelium compromised membrane integrity and nutrient assimilation, contributing to growth arrest. Similar oxidative stress–driven performance loss has been reported in Hessian fly on resistant wheat and *Myzus persicae* on resistant potato (Mittapalli et al. 2007; Rigsby et al. 2015; Quandahor et al. 2022). Additionally, upregulation of inhibitors of apoptosis proteins (IAPs) in resistant-fed larvae suggested incomplete suppression of stress-induced apoptosis (Zhang et al. 2019b), while downregulation of juvenile hormone binding protein (JHBP) implied hormonal imbalance disrupting larval development.

Together, these findings demonstrate that resistant chickpea genotypes impose a multifaceted stress regime on *H. armigera*—detoxification overload, oxidative stress, digestive disruption, and endocrine imbalance (War et al. 2012; Zhou et al. 2019; Li et al. 2022; Chamani et al. 2025). Conversely, larvae on susceptible genotypes encounter a permissive biochemical environment that supports efficient metabolism and development. These insights highlight the utility of proteomics in unraveling host resistance mechanisms and their cascading effects on insect physiology.

Functional validation of linoleic acid involved in the JA signaling pathway

Upon herbivore attack, membrane lipids are cleaved by phospholipases to release polyunsaturated fatty acids, primarily linoleic acid (18:2) and linolenic acid (18:3) (Conconi et al. 1996; Qi et al. 2011). Linoleic acid serves as a precursor of bioactive oxylipins, while its desaturation to linolenic acid initiates the octadecanoid pathway leading to JA synthesis (Nishizato et al. 2025). Through sequential action of 13-LOX, AOS, and AOC, linolenic acid is converted to JA, a central defense hormone that induces protease inhibitors, secondary metabolites, and other herbivore responses (Nishizato et al. 2025; Hunter et al. 2025). Thus, fatty acids—especially linoleic and linolenic acids—form the biochemical bridge linking membrane lipid turnover to JA-mediated plant resistance.

The *In-silico* analyses suggest that *H. armigera* CYP450s can potentially interact with linoleic acid (LA), with docking and molecular dynamics indicating a stable LA–CYP450 complex oriented for catalysis. Similar to vertebrate CYP2J/2C enzymes that generate 9,10- and 12,13-epoxyoctadecenoic acids (EpOMEs), insect CYP450s may have the capacity to convert dietary or membrane-derived LA into EpOMEs (Vatanparast et al. 2020). EpOMEs have been reported as potent physiologically active oxylipins with immunomodulatory effects. In *Spodoptera exigua* and *Maruca vitrata*, 12,13-EpOME suppressed hemocyte spreading, nodulation, phenoloxidase activity, and antimicrobial peptide induction, while inhibition of soluble epoxide hydrolase (sEH) prolonged EpOME activity and increased pathogen susceptibility (Shahmohammadi et al. 2025). These findings indicate that LA-derived EpOMEs can act as modulators of modulators of insect physiological responses.

Bioassays further support this interpretation. LA showed only moderate toxicity against *H. armigera* larvae, consistent with the metabolism-dependent enhancement of toxicity. However, EpOME analogs or stabilized derivatives were markedly more potent, reducing larval growth and development. These observations suggest that LA may function as a potential pro-toxin, although direct in vivo evidence for its metabolic conversion into EpOMEs within the insect was not obtained in the present study. Accordingly, the proposed "Trojan horse" mechanism—where plant-derived LA is metabolically activated by insect CYP450s into more toxic oxylipins—should be considered a working hypothesis supported by correlative evidence from proteomics, computational analysis, and larval bioassays rather than a confirmed pathway. Importantly, EpOME or other oxidized LA metabolites were not directly detected in larval tissues or gut contents in this study. Targeted metabolomic analysis will be required to confirm the in vivo formation of these metabolites under physiological feeding conditions. Furthermore, while docking and molecular dynamics analyses indicate structural compatibility and binding potential, experimental validation through enzyme activity assays or CYP450 inhibition studies will be necessary to establish metabolism-dependent toxicity. The bioassays conducted measured larval mortality and growth effects only; therefore, any potential impact of LA-derived metabolites on insect immune function remains hypothetical and was not directly assessed. This strategy offers a potential basis for HPR mechanism, distinct from neurotoxic or endocrine-targeting insecticides, and highlights the potential of LA derivatives and EpOME mimics in sustainable pest management.

Conclusion

Plant–insect interactions reflect a continuous molecular arms race. In this dynamic, resistant chickpea genotypes mount JA-dependent defenses through secondary metabolites, resistance proteins, and biochemical barriers, while *H. armigera* counters via detoxification enzymes, proteolytic adjustments, and behavioral shifts. Proteomic evidence demonstrates that chickpea deploys a hierarchical defense protein network capable of neutralizing insect midgut proteases. In turn, larvae feeding on resistant genotypes experience oxidative stress–driven trade-offs that impair survival and fitness. The present findings represent an early defense response captured at 24 h after

infestation, and future time-course studies will be required to fully understand the temporal dynamics of resistance mechanisms. Furthermore, linoleic acid (LA) showed larval toxicity and is suggested to function as a potential pro-toxin, although the metabolic conversion of LA into more active derivatives within the insect remains to be experimentally validated. The proposed involvement of LA-derived oxylipins in modulating insect physiological processes should therefore be considered a hypothesis supported by correlative evidence rather than a confirmed mechanism. Overall, the integrated host–pest proteomic analysis revealed that resistant chickpea and its crop wild relative exhibit enhanced early signaling, transcriptional reprogramming, lipid-mediated defense, and constitutive biochemical barriers that collectively restrict larval performance. These responses highlight the biological significance of early JA-associated signaling and lipid-derived defense pathways as key components of effective resistance. These multilayered responses underscore the complexity of chickpea–*H. armigera* interactions and reveal strategic molecular targets for crop protection. The identified defense-associated proteins and lipid-mediated pathways provide potential biomarkers and candidate traits for resistance breeding and integrated pest management. Importantly, the resistance-linked proteins and pathways identified in the crop wild relative represent valuable molecular resources for introgression and marker-assisted selection to broaden the genetic base of cultivated chickpea. Harnessing natural variation in defense metabolites, alongside enhancing early activation of the JA pathway through molecular breeding, represents a promising approach for the development of insect-resilient chickpea cultivars.

Supplementary Information The online version contains supplementary material available at https://doi.org/10.1007/s00299-026-03763-3.

Acknowledgements The authors acknowledge Punjab Agricultural University (PAU), India for supplying the chickpea genotypes. We also thank Genebank-ICRISAT, Hyderabad, for providing chickpea crop wild relatives. We extend our gratitude to Hemalatha Sanivarapu, Rajendra Badbadwal, Venkata Ramana, and Rajendra Prasad for their extensive support and assistance during the field and laboratory experiments.

Author contributions Gothe Revanayya: Writing—original draft, Laboratory experiments, Writing—review & editing, Methodology, Formal analysis, Visualization, Funding acquisition, Data curation. Inderjit Singh: Methodology, Writing—original draft, Writing—review & editing, Supervision. Onkarappa Dhanyakumar: Writing—original draft, Visualization, laboratory experiments, Validation, Methodology, Data curation, Writing—review & editing. Jagdish Jaba: Writing—review & editing, Validation, Supervision, Resources, Methodology, Investigation, Funding acquisition, Data curation, Conceptualization. Dharminder Bhatia: Writing—review & editing, Data curation. Shayla Bindra: Writing—review & editing, Data curation, Conceptualization. Ravinder Singh: Laboratory experiments, Validation, Methodology, Writing—review & editing. Himabindu Kudapa: Writing—review & editing, Data curation, Conceptualization. Kalenahalli Yogendra: Writing—review & editing, Validation, Supervision, Resources, Methodology, Investigation, Conceptualization.

Funding Gothe Revanayya is thankful to the Department of Science and Technology, Government of India, for SERB-CII Prime Minister's fellowship for doctoral research support. Onkarappa Dhanyakumar is supported by the University Grants Commission (UGC) fellowship (ID: 2021–22-KAR-10322), Government of India, for his doctoral research. Jagdish Jaba and Kalenahalli Yogendra thankful for other donors like DST-YSS/2015/000673/LS, ICAR-ICRISAT & VAC's funded through USAID collaborative projects for conducting host plant resistance studies on pigeonpea crop.

Data availability All proteomics raw data generated in this study have been deposited in ProteomeXchange under accession number-PXD068327. All other relevant data are included within the article and its supplementary materials.

Declarations

Conflict of interest The authors declare no known competing financial interests or personal relationships that could have influenced the work reported in this paper.

References

Aboua LR, Seri-Kouassi BP, Koua HK (2010) Insecticidal activity of essential oils from three aromatic plants on *Callosobruchus maculatus* F. in Côte D'ivoire. Eur J Sci Res 39:243–250

Ali MR, Uemura T, Ramadan A et al (2019) The ring-type E3 ubiquitin ligase JUL1 targets the VQ-motif protein JAV1 to coordinate jasmonate signaling. Plant Physiol 179:1273–1284

Ali J, Tona A, Islam T et al (2024) Defense strategies and associated phytohormonal regulation in Brassica plants in response to chewing and sap-sucking insects. Front Plant Sci 15:1376917

Arimura G, Tashiro K, Kuhara S et al (2000) Gene responses in bean leaves induced by herbivory and by herbivore-induced volatiles. Biochem Biophys Res Commun 277:305–310

Avuthu T, Sanivarapu H, Prasad K et al (2024) Comparative metabolomics analysis reveals secondary cell wall thickening as a barrier to resist *Aspergillus flavus* infection in groundnut. Physiol Plant 176:14169

Benjamini Y, Hochberg Y (1995) Controlling the false discovery rate: a practical and powerful approach to multiple testing. J R Stat Soc Ser B Stat Methodol 57:289–300. https://doi.org/10.1111/j.2517-6161.1995.tb02031.x

Bhatnagar MP, Yogendra K, Parankusam S et al (2021) Comparative proteomics provide insights on the basis of resistance to *Aspergillus flavus* infection and aflatoxin production in peanut (*Arachis hypogea* L.). J Plant Interact 16:494–509. https://doi.org/10.1080/17429145.2021.1995058

Bhattacharjee M, Dhar S, Handique PJ et al (2020) Defense response in chickpea pod wall due to simulated herbivory unfolds differential proteome profile. Protein J 39:240–257

Bonaventure G, Schuck S, Baldwin IT (2011) Revealing complexity and specificity in the activation of lipase?mediated oxylipin biosynthesis: a specific role of the *Nicotiana attenuata* GLA1 lipase in the activation of jasmonic acid biosynthesis in leaves and roots. Plant Cell Environ 34:1507–1520

Castañeda LE, Figueroa CC, Fuentes-Contreras E et al (2009) Energetic costs of detoxification systems in herbivores feeding on

chemically defended host plants: a correlational study in the grain aphid, *Sitobion avenae*. J Exp Biol 212:1185–1190
Celorio-Mancera MDLP, Courtiade J, Muck A et al (2011) Sialome of a generalist lepidopteran herbivore: identification of transcripts and proteins from *Helicoverpa armigera* labial salivary glands. PLoS ONE 6:e26676
Chamani M, Dadpour M, Dehghanian Z et al (2025) From digestion to detoxification: exploring plant metabolite impacts on insect enzyme systems for enhanced pest control. Insects 16:392
Cheah BH, Lin HH, Chien HJ et al (2020) SWATH-MS-based quantitative proteomics reveals a uniquely intricate defense response in *Cnaphalocrocis medinalis*-resistant rice. Sci Rep 10:6597
Chen MS (2008) Inducible direct plant defense against insect herbivores: a review. Insect Sci 15:101–114
Chen L, Song J, Wang J et al (2023) Effects of methyl jasmonate fumigation on the growth and detoxification ability of *Spodoptera litura* to xanthotoxin. Insects 14:145
Chujo T, Miyamoto K, Ogawa S et al (2014) Overexpression of phosphomimic mutated OsWRKY53 leads to enhanced blast resistance in rice. PLoS ONE 9:98737
Conconi A, Miquel M, Browse JA, Ryan CA (1996) Intracellular levels of free linolenic and linoleic acids increase in tomato leaves in response to wounding. Plant Physiol 111:797–803
Erb M, Reymond P (2019) Molecular interactions between plants and insect herbivores. Annu Rev Plant Biol 70:527–557
Francis F, Vanhaelen N, Haubruge E (2005) Glutathione S-transferases in the adaptation to plant secondary metabolites in the *Myzus persicae* aphid. Arch Insect Biochem Physiol 58:166–174
Gatehouse JA (2002) Plant resistance towards insect herbivores: a dynamic interaction. New Phytol 156:145–169
Golla SK, Rajasekhar P, Akbar SMD, Sharma HC (2018a) Proteolytic activity in the midgut of *Helicoverpa armigera* (Noctuidae: Lepidoptera) larvae fed on wild relatives of chickpea, *Cicer arietinum*. J Econ Entomol 111:2409–2415
Golla SK, Rajasekhar P, Sharma SP et al (2018b) Antixenosis and antibiosis mechanisms of resistance to pod borer, *Helicoverpa armigera* in wild relatives of chickpea, *Cicer arietinum*. Euphytica 214:1–16
Golla SK, Sharma HC, Rajasekhar P et al (2020) Biochemical components of wild relatives of chickpea confer resistance to pod borer, *Helicoverpa armigera*. Arthropod-Plant Interact 14:623–639
Gothe RM, Karrem A, Gowda RSR et al (2024) Decoding plant defense: accelerating insect pest resistance with omics and high-throughput phenotyping. Plant Physiol Rep 29:793–807. https://doi.org/10.1007/s40502-024-00835-y
Gowda CLL, Lateef SS, Smithson JB, Reed W (1983) Breeding for resistance to Heliothis armigera in chickpea. In: Proceedings of the National seminar on breeding crop plants for resistance to pests and diseases, School of Genetics. Tamil Nadu Agricultural University Coimbatore, Tamil Nadu, India
Ha EM, Lee KA, Seo YY et al (2009) Coordination of multiple dual oxidase-regulatory pathways in responses to commensal and infectious microbes in *Drosophila* gut. Nat Immunol 10:949
Heilmann I (2016) Plant phosphoinositide signaling-dynamics on demand. Biochim Biophys Acta BBA-Mol Cell Biol Lipids 1861:1345–1351. https://doi.org/10.1016/j.bbalip.2016.02.013
Hu L, Ye M, Kuai P et al (2018) OsLRR-RLK1, an early responsive leucine-rich repeat receptor-like kinase, initiates rice defense responses against a chewing herbivore. New Phytol 219:1097–1111
Hunter CT, Gorman Z, Li Q et al (2025) Disruption of allene oxide cyclase in maize reveals the necessity of enzymatically produced 12- OPDA for the induction of jasmonic acid during herbivory. Plant J 122:e70209. https://doi.org/10.1111/tpj.70209
Jaba J, Devrani A, Agnihotri M, Chakravarty S (2017) Screening of chickpea cultivars against pod borer *Helicoverpa armigera* (Hubner) under unprotected conditions. J Exp Zool India 20:835–843
Jaba J, Bhandi S, Deshmukh S et al (2021) Identification, Evaluation and Utilization of Resistance to Insect Pests in Grain Legumes: Advancement and Restrictions. In: Saxena KB, Saxena RK, Varshney RK (eds) Genetic Enhancement in Major Food Legumes. Springer International Publishing, Cham, pp 197–230
Jiang Q, Ding C, Feng L et al (2025) Two leucine-rich repeat receptor-like kinases initiate herbivory defense responses in tea plants. Hortic Res 12:281
Jones RM, Luo L, Ardita CS et al (2013) Symbiotic *lactobacilli* stimulate gut epithelial proliferation via Nox mediated generation of reactive oxygen species. EMBO J 32:3017–3028
Kandoth PK, Ranf S, Pancholi SS et al (2007) Tomato MAPKs LeMPK1, LeMPK2, and LeMPK3 function in the systemin-mediated defense response against herbivorous insects. Proc Natl Acad Sci U S A 104:12205–12210
Kawaguchi J, Hayashi K, Desaki Y et al (2023) JUL1, ring-type E3 ubiquitin ligase, is involved in transcriptional reprogramming for ERF15-mediated gene regulation. Int J Mol Sci 24:987
King AM, MacRae TH (2015) Insect heat shock proteins during stress and diapause. Annu Rev Entomol 60:59–75
Kuroda R, Kato M, Tsuge T, Aoyama T (2021) *Arabidopsis* phosphatidylinositol 4-phosphate 5-kinase genes PIP5K7, PIP5K8, and PIP5K9 are redundantly involved in root growth adaptation to osmotic stress. Plant J 106:913–927
Lawrence SD, Novak NG (2018) Over-expression of StZFP2 in *Solanum tuberosum* L. Plant Signal Behav 13:1489668
Li R, Zhang J, Li J et al (2015) Prioritizing plant defence over growth through WRKY regulation facilitates infestation by non-target herbivores. Elife 4:04805
Li AM, Wang M, Chen ZL et al (2022) Integrated transcriptome and metabolome analysis to identify sugarcane gene defense against fall armyworm (*Spodoptera frugiperda*) herbivory. Int J Mol Sci 23:13712
Livak KJ, Schmittgen TD (2001) Analysis of relative gene expression data using real-time quantitative PCR and the 2- ΔΔCT method. Methods 25:402–408
Lomate PR, Sangole KP, Sunkar R, Hivrale VK (2015) Superoxide dismutase activities in the midgut of *Helicoverpa armigera* larvae: identification and biochemical properties of a manganese superoxide dismutase. Open Access Insect Physiol 13–20
Machado RA, Robert CA, Arce CC et al (2016) Auxin is rapidly induced by herbivore attack and regulates a subset of systemic, jasmonate dependent defenses. Plant Physiol 172:521–532
Meshram S, Das D, Singh S et al (2025) Dynamics of cytosolic and organellar gene transcripts in wild and cultivated genotypes of pigeon pea due to simulated herbivory. Plant Sci 357:112537
Mittapalli O, Neal JJ, Shukle RH (2007) Antioxidant defense response in a galling insect. Proc Natl Acad Sci U S A 104:1889–1894
Mulla JA, Tamhane VA (2023) Novel insights into plant defensin ingestion induced metabolic responses in the polyphagous insect pest *Helicoverpa armigera*. Sci Rep 13:3151
Napoleão TH, Albuquerque LP, Santos ND et al (2019) Insect midgut structures and molecules as targets of plant-derived protease inhibitors and lectins. Pest Manag Sci 75:1212–1222
Narayanamma VL, Gowda CLL, Sriramulu M et al (2013) Nature of gene action and maternal effects for pod borer; *Helicoverpa armigera* resistance and grain yield in chickpea; *Cicer arietinum*. Am J Plant Sci 4:26–33
Ngugi-Dawit A, Njaci I, Higgins TJ et al (2021) Comparative TMT proteomic analysis unveils unique insights into *Helicoverpa armigera* (Hübner) resistance in *Cajanus scarabaeoides* (L.) Thouars. Int J Mol Sci 22:5941

Nishizato Y, Okumura T, Matsumoto K, Ueda M (2025) Recent advances in the chemistry and biology of plant oxylipin hormones. Nat Prod Rep. https://doi.org/10.1039/d5np00006h

Pandey SP, Srivastava S, Goel R et al (2017) Simulated herbivory in chickpea causes rapid changes in defense pathways and hormonal transcription networks of JA/ethylene/GA/auxin within minutes of wounding. Sci Rep 7:44729

Pavithran S, Murugan M, Yogendra K et al (2024) Proteomic insights into the saliva and salivary glands of the cotton aphid, *Aphis gossypii* (Hemiptera: Aphididae. Phytoparasitica 52:73

Pitzschke A (2015) Modes of MAPK substrate recognition and control. Trends Plant Sci 20:49–55

Qi J, Zhou G, Yang L et al (2011) The chloroplast-localized phospholipases D α4 and α5 regulate herbivore-induced direct and indirect defenses in rice. Plant Physiol 157:1987–1999

Quandahor P, Gou Y, Lin C, Liu C (2022) Potato (*Solanum tuberosum* L.) leaf extract concentration affects performance and oxidative stress in green peach aphids (*Myzus persicae* (Sulzer). Plants 11:2757

Rigsby CM, Showalter DN, Herms DA et al (2015) Physiological responses of emerald ash borer larvae to feeding on different ash species reveal putative resistance mechanisms and insect counteradaptations. J Insect Physiol 78:47–54

Rodriguez MC, Petersen M, Mundy J (2010) Mitogen-activated protein kinase signaling in plants. Annu Rev Plant Biol 61:621–649

Rustagi A, Chugh S, Sharma S, et al (2021) Plant-insect interaction: a proteomic approach in defence mechanism. In: Plant-pest interactions: From molecular mechanisms to chemical ecology: Chemical ecology. pp 57–72

Schmelz EA, Alborn HT, Tumlinson JH (2003) Synergistic interactions between volicitin, jasmonic acid and ethylene mediate insect?induced volatile emission in *Zea mays*. Physiol Plant 117:403–412

Schweizer F, Bodenhausen N, Lassueur S et al (2013) Differential contribution of transcription factors to *Arabidopsis thaliana* defense against *Spodoptera littoralis*. Front Plant Sci 4:13

Shahmohammadi N, Haraji S, Khan F et al (2025) Antagonistic control of intracellular signals by EpOMEs in hemocytes induced by PGE2 and their chemical modification for a potent insecticide. PLoS ONE 20:0320488

Sharma HC, Gowda CLL, Stevenson PC et al (2007) Host plant resistance and insect pest management. In: Yadav SS, Redden R, Chen W, Sharma B (eds) Chickpea breeding and management. CAB International, Oxford, pp 520–537

Singh M, Malhotra N, Singh K (2021) Broadening the genetic base of cultivated chickpea following introgression of wild *Cicer* species-progress, constraints and prospects. Genet Resour Crop Evol 68:2181–2205

Somers DA, Samac DA, Olhoft PM (2003) Recent advances in legume transformation. Plant Physiol 131:892–899

Tamhane VA, Sant SS, Jadhav AR et al (2021) Label-free quantitative proteomics of *Sorghum bicolor* reveals the proteins strengthening plant defense against insect pest *Chilo partellus*. Proteome Sci 19:6

Varsani S, Grover S, Zhou S et al (2019) 12-Oxo-phytodienoic acid acts as a regulator of maize defense against corn leaf aphid. Plant Physiol 179:1402–1415

Vatanparast M, Ahmed S, Lee DH et al (2020) EpOMEs act as immune suppressors in a lepidopteran insect, *Spodoptera exigua*. Sci Rep 10:20183

Vos M, Denekamp M, Dicke M et al (2006) The *Arabidopsis thaliana* transcription factor AtMYB102 functions in defense against the insect herbivore Pieris rapae. Plant Signal Behav 1:305–311

Wang C, Zien CA, Afitlhile M et al (2000) Involvement of phospholipase D in wound-induced accumulation of jasmonic acid in *Arabidopsis*. Plant Cell 12:2237–2246

Wang Q, Li J, Hu L et al (2013) OsMPK3 positively regulates the JA signaling pathway and plant resistance to a chewing herbivore in rice. Plant Cell Rep 32:1075–1084

War AR, Paulraj MG, Ahmad T et al (2012) Mechanisms of plant defense against insect herbivores. Plant Signal Behav 7:1306–1320

War WA, Rasool J, Bhat AA et al (2024) An overview of the biological aspects, nature of damage and strategies for managing the gram pod borer (*Helicoverpa armigera* Hubner) in chickpea: a review. J Sci Res Rep 30:643–659

Wu J, Baldwin IT (2010) New insights into plant responses to the attack from insect herbivores. Annu Rev Genet 44:1–24

Wu J, Hettenhausen C, Meldau S (2007) Herbivory rapidly activates MAPK signaling in attacked and unattacked leaf regions but not between leaves of *Nicotiana attenuata*. Plant Cell 19:1096–1122

Yao DM, Zou C, Shu YN, Liu SS (2020) WRKY transcription factors in *Nicotiana tabacum* modulate plant immunity against whitefly via interacting with MAPK cascade pathways. Insects 12:16

Yogendra KN, Dhokane D, Kushalappa AC et al (2017) StWRKY8 transcription factor regulates benzylisoquinoline alkaloid pathway in potato conferring resistance to late blight. Plant Sci 256:208–216

Yu SJ, Hsu EL (1993) Induction of detoxification enzymes in phytophagous insects: role of insecticide synergists, larval age, and species. Arch Insect Biochem Physiol 24:21–32

Zhai Y, Li P, Mei Y et al (2017) Three MYB genes co-regulate the phloem-based defence against English grain aphid in wheat. J Exp Bot 68:4153–4169

Zhang H, Yasmin F, Song BH (2019a) Neglected treasures in the wild-legume wild relatives in food security and human health. Curr Opin Plant Biol 49:17–26

Zhang W, Liang G, Ma L et al (2019b) Dissecting the role of juvenile hormone binding protein in response to hormone and starvation in the cotton bollworm, *Helicoverpa armigera* (Hübner. J Econ Entomol 112:1411–1417

Zhang X, Wang X, Wang T (2024) Comprehensive transcriptomic analysis reveals defense-related genes and pathways of rice plants in response to Fall Armyworm (*Spodoptera frugiperda*) infestation. Plants 13:2879

Zheng R, Xia Y, Keyhani NO (2021) Differential responses of the antennal proteome of male and female migratory locusts to infection by a fungal pathogen. J Proteomics 232:104050

Zheng S, Luo J, Zhu X et al (2022) Transcriptomic analysis of salivary gland and proteomic analysis of oral secretion in *Helicoverpa armigera* under cotton plant leaves, gossypol, and tannin stresses. Genomics 114:110267

Zhou Z, Zhao Y, Bi G et al (2019) Early signalling mechanisms underlying receptor kinase-mediated immunity in plants. Philos Trans R Soc Lond B Biol Sci 374:20180310

Authors and Affiliations

Gothe Revanayya[1,2] · Inderjit Singh[1] · Onkarappa Dhanyakumar[2,3] · Jagdish Jaba[2] · Dharminder Bhatia[1] · Shayla Bindra[1] · Ravinder Singh[1] · Himabindu Kudapa[2] · Kalenahalli Yogendra[2]

✉ Jagdish Jaba
Jagdish.Jaba@icrisat.org

✉ Kalenahalli Yogendra
Yogendra.Kalenahalli@icrisat.org

Gothe Revanayya
revanayya-pbg@pau.edu

Inderjit Singh
inderjitpb@pau.edu

Onkarappa Dhanyakumar
dhanyakumarento@gmail.com

Dharminder Bhatia
d.bhatia@pau.edu

Shayla Bindra
shaylabindra@pau.edu

Ravinder Singh
ravindergurwara@pau.edu

Himabindu Kudapa
Himabindu.Kudapa@icrisat.org

1 Department of Plant Breeding and Genetics, Punjab Agricultural University, Ludhiana 141004, Punjab, India

2 International Crops Research Institute for the Semi-Arid Tropics, Patancheru, Hyderabad 502324, Telangana, India

3 Department of Agricultural Entomology, Tamil Nadu Agricultural University, Coimbatore 641003, Tamil Nadu, India